2007 IEEE International Conference on
Robotics and Automation
Roma, Italy, 10-14 April 2007

Force Redistribution in a Quadruped Running Trot

Luther R. Palmer III
Department of Electrical and Computer Engineering
The Ohio State University
Columbus, Ohio 43210
Email: palmer.216@osu.edu

David E. Orin
Department of Electrical and Computer Engineering
The Ohio State University
Columbus, Ohio 43210
Email: orin.1@osu.edu

***Abstract*— In this paper, an attitude control strategy is developed for a high-speed quadruped trot. The forces in the trot are redistributed among the legs to stabilize the pitch and roll of the system. An important aspect of the strategy is that the controller works to preserve the passive dynamics of quadruped trotting that are accurately predicted by the spring-loaded inverted pendulum (SLIP) model. A hybrid control strategy is presented which allows the quadruped to reach a speed of $4.75\ m/s$ and turn at a rate of $20\ deg/s$ in simulation under operator control. The *discrete* part of the controller runs once per trot step and outputs a stance thrust energy and hip angles for touchdown. The stance thrust energy accounts for losses during the step, especially at touchdown. Both the stance thrust energy and hip angles dictate the natural dynamics during stance. The force redistribution algorithm *continuously* operates during stance to stabilize the body's tilt axes, roll and pitch, with minimal effect on the prescribed natural dynamics. The $1.0\ m/s$ increase in speed over previously presented work is largely due to the more dynamically-consistent force redistribution algorithm presented in this paper. The controller also tracks desired changes in heading, for which the biomimetic method of banking into a high-speed turn is also realized.**

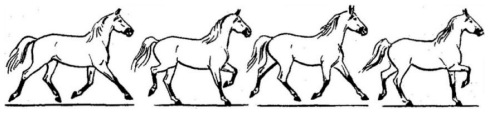

Fig. 1. Trotting stride showing two stance phases interleaved with two flight phases. The quadruped is largely uncontrollable during flight [6].

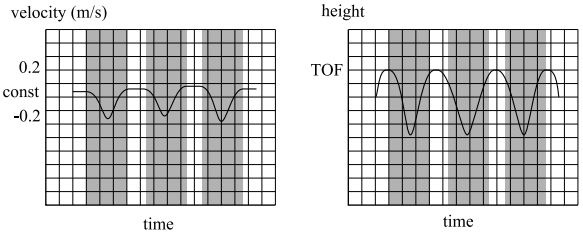

Fig. 2. Fore-aft and vertical oscillations during steady state running, adapted from [7]. During periods of foot-ground contact (shaded), the legs reverse the body's vertical momentum and supply braking and accelerating forces in the fore-aft direction.

I. Introduction

Cheetahs running at high speed over unprepared terrain and dogs navigating dense wreckage for search and rescue are only two of the many remarkable performances that legged robots will emulate in the future, but the problem of high-speed legged locomotion has proven difficult to solve. Aside from trying to mimic the small yet powerful actuators and the precise and high-bandwidth sensing systems that animals employ, understanding and implementing the control mechanisms that animals use to robustly navigate uneven terrain at high speeds remains an unsolved problem.

The goal of this paper is to present a useful control strategy for a 3-dimensional (3D) running trot. The trot was chosen because of its observed energy efficiency over a wide range of running speeds [1] and its widespread use in nature [2]. The trot, as shown in Fig. 1, is a symmetric gait during which the diagonal forelimb and hindlimb move in unison, ideally contacting and leaving the ground at the same time. Bounding algorithms have been studied [3], [4], but very few animals naturally bound due in part to its higher energy cost per stride when compared to trotting [5].

Figure 2 shows representative data taken for a dog trotting at a constant speed [7]. During the periods of foot-ground contact, which are shaded in the figure, the leg forces supply braking and accelerating forces in the fore-aft direction while also reversing the body's vertical momentum. The apex of the flight phase is labeled as the top of flight (TOF). The forward and vertical motions of the body's center of gravity are in phase during running and are similar to that of a simple spring-mass system such as a person jumping on a pogo stick [7], [8]. A linear spring in the leg represents the elastic characteristics of the musculoskeletal system and the mass is equivalent to the mass of the animal. The spring-mass model, or spring-loaded inverted pendulum (SLIP) model, has been shown to describe and predict the mechanics of quadruped trotters remarkably well [9], [10].

The SLIP model describes the passive dynamics of a quadruped running trot. It has been suggested that an active control law that closely mimics a passive system is likely to enjoy certain advantages of the passive system such as energy optimality and stability [11]. Based on this assumption, the controller presented in this paper seeks to preserve the passive dynamics of quadruped trotting while running at high speeds. Although a study of energy optimality will be the focus of future work, this controller stabilizes the quadruped trot well enough at high speeds to handle the added difficulty of turning. The top speed of the quadruped under this control is $4.75\ m/s$ and the maximum turning rate is $20\ deg/s$.

1-4244-0602-1/07/$20.00 ©2007 IEEE.

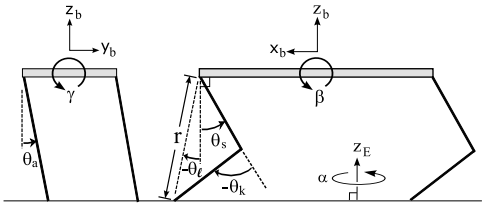

Fig. 3. Body model and leg kinematics.

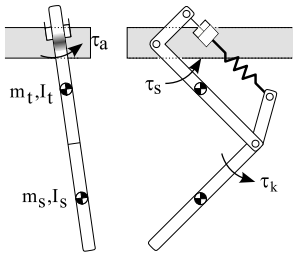

Fig. 4. Dynamic leg model.

Raibert [3] employed the use of compliant elements in the legs to experimentally trot, bound, and pace. The pitch controller could not eliminate a significant nose-down attitude during steady-state running and only a rough relationship existed between the desired and actual forward running speeds. The maximum speed achieved was $2.2\ m/s$ and although a forward heading was maintained, this algorithm did not track changes in desired heading. Herr and McMahon [12] stabilized a trot in numerical simulation by using hip torque to control both forward velocity and pitch. This system was planar (no turning) and the controller was only tested at 4 discrete velocities between $2.2\ m/s$ and $4.4\ m/s$ and was never shown to track regular changes in desired velocity.

This paper is organized as follows. The quadruped model is presented in Section II, followed by the presentation of the hybrid control approach for trotting in Section III. The simulation results of the controller are shown in Section IV, and are followed by a summary and discussion of future work.

II. Quadruped Model

A model of the 3D quadruped system used in this work is shown in Fig. 3. A dynamic model of the leg is shown in Fig. 4. The legs each have two actuators at the shoulder/hip joints, one for abduction and adduction of the leg and another to swing (protract/retract) the leg. The resultant leg angles are θ_a and θ_s, respectively. The abduction and adduction actuators and axes will hereafter be referred to as "ab/ad". A third actuator on the thigh adjusts the rest position of a series spring element. The resulting force acts at the knee to adjust the virtual leg length, r, during flight and can continuously adjust the spring length during stance to add or remove energy from the system. Energy is stored in the spring as the knee bends during the first half of stance and is returned to the system as the leg lengthens. The energy conserved by the spring reduces the effort required to maintain a consistent height from step to step. The angle of the knee is θ_k, and the angle of the virtual leg with respect to the body normal is θ_ℓ.

Figure 3 shows the specific body angles to be controlled: roll, γ, pitch, β, and yaw, α, along with the forward velocity, v_b^x, lateral velocity, v_b^y, and height, $h = p_E^z$, at the top of flight (TOF). A step starts at a TOF and concludes at the next TOF, with a diagonal leg pair having contacted the ground and exerted an appropriate impulse during that time.

The quadruped weighs a total of $68\ kg$ and stands $60\ cm$ high with the knee springs in their nominal position. The shoulder separation is $35\ cm$ and the shoulder-to-hip distance is $1.2\ m$. The dimensions were chosen to match those of a mid-sized goat. The thigh and shank are modeled as slim rods of length $35\ cm$ with geometrically-centered masses of $1.0\ kg$. The spring constant is fixed at $25,820\ N/m$. A full set of system parameters is presented in [13].

The control algorithm developed in the next section is designed for a wide range of body scales and leg configurations. The algorithm solves for knee torques, τ_k, swing torques, τ_s, and ab/ad torques, τ_a, which can be resolved by many different spring/actuator configurations on each joint.

III. Control Approach

A key goal of this work is to develop a controller for high-speed trotting which preserves the natural dynamics observed in nature and predicted by the SLIP model. Understanding the SLIP model leads to heuristic control principles such as adjusting the touchdown position of the feet with respect to their hips to control the fore-aft velocity, placing the legs in scissor-like positions at touchdown to cause yaw moments during stance, and increasing the magnitude of the leg forces during stance to raise the height of the body at TOF.

The SLIP model, however, does not yield general principles for controlling the body's pitch and roll. Biomechanics studies show that pitch stability for the quadruped trot is achieved by redistributing the vertical impulses during stance between the fore and hind limbs [14]. This principle will be used in our control approach. In particular, the controller seeks to redistribute the leg forces to simultaneously stabilize pitch and roll without affecting the natural dynamics of the forward, lateral, vertical, and yaw motions.

With two feet in point contact with the ground, no moment can be exerted on the system about the line connecting the two feet [15]. Any of the six body motions can be controlled, but potentially at the expense of the others. The fast response of the pitch and roll motions during stance require that their control be given priority to maintain a sustainable gait.

The control system, as shown in Fig. 5, is divided into two parts: a step controller run once per step which dictates a nominally passive motion during stance to control forward, lateral, vertical and yaw motions, and the force redistribution during stance which stabilizes pitch and roll with minimal

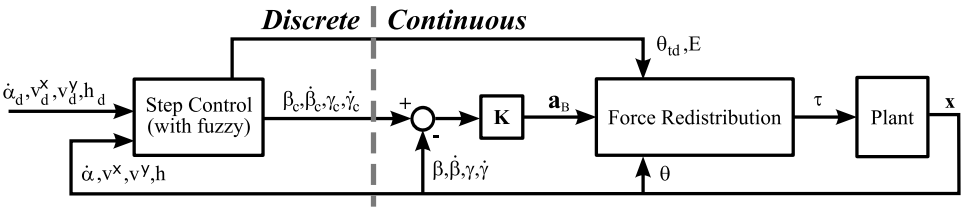

Fig. 5. Attitude control system. Yaw rate ($\dot{\alpha}$), forward velocity (v^x), lateral velocity (v^y), and height (h) are tracked through the step controller which runs once per step while pitch (β) and roll (γ) are regulated through continuous force redistribution during stance.

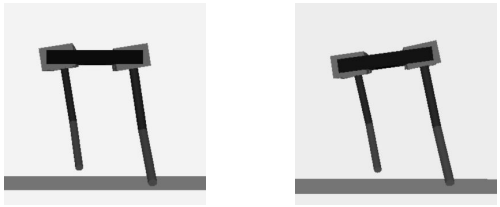

(a) Flat turn. (b) Banked turn.

Fig. 6. Turning with and without body roll.

effect on the prescribed passive motion. Both are described below.

A. Step Control

This aspect of the control system remains largely unchanged from earlier work [16]. Forward and lateral velocity are controlled by varying the virtual leg angles and ab/ad angles for touchdown. Yaw rate is controlled by the difference in touchdown ab/ad angles between the fore and hind limb. Vertical height is controlled during stance by an instantaneous thrust when the leg is maximally compressed. These control principles were successfully used by Raibert [3], but a fuzzy controller is implemented to improve the performance of the quadruped by computing the leg angles and thrust values. Once per step, at TOF, the fuzzy controller receives as its inputs the desired turning rate, $\dot{\alpha}_d$, desired forward velocity, v_d^x, desired lateral velocity (always zero), v_d^y, desired height, h_d, and the present body state, $\boldsymbol{x}$. The controller outputs a set of desired leg touchdown angles, $\boldsymbol{\theta}_{td}$, and the amount of energy, E, that will be added to each knee spring during the next support phase. A formal discussion of the fuzzy controller is not presented here because of space considerations, but is described in [13].

The step controller also outputs a commanded pitch, β_c, pitch rate, $\dot{\beta}_c$, roll, γ_c, and roll rate, $\dot{\gamma}_c$, for the body to achieve during stance. The commanded pitch and pitch rate are nominally zero, but the pitch can be changed to match the inclination angle on sloped terrain. Animals have been observed to bank into turns, as shown in Fig. 6, to keep their ab/ad angles with respect to the body small. The computation of this bank angle is described in earlier work [16]. Simply stated, the body's roll angle is directly proportional to both velocity and turning rate.

B. Force Redistribution

The passive motions predicted by the SLIP model will be called the SLIP motions and include forward, lateral, vertical, and yaw motions. Tilt motions, roll and pitch, will be controlled by the continuous force redistribution algorithm during stance. This algorithm attempts to solve for the joint torques of the stance legs that servo the body's tilt motions to their desired positions without disturbing the SLIP motions. From Fig. 5, the force redistribution controller calculates the joint torques, $\boldsymbol{\tau}$, to produce the desired body accelerations, $\mathbf{a}_B$. This is a change from our previous work [17], in which desired body forces were solved for without accounting for the inertial effects of the legs. This algorithm is more dynamically accurate and stabilizes the trot at higher speeds than previously capable.

The torque of leg ℓ, $\boldsymbol{\tau}_\ell$, consists of the ab/ad, swing, and knee torque respectively as

$$\boldsymbol{\tau}_\ell = [\tau_{\ell,a},\ \tau_{\ell,s},\ \tau_{\ell,k}]^T \qquad \ell = 1,2,3,4\ . \tag{1}$$

The articulated body (AB) algorithm, outlined in [18], [19], for the formulation of legged robot dynamics relates the body's acceleration, $\mathbf{a}_B = [\mathrm{a}_B^\gamma,\ \mathrm{a}_B^\beta,\ \mathrm{a}_B^\alpha,\ \mathrm{a}_B^x,\ \mathrm{a}_B^y,\ \mathrm{a}_B^z]^T$, as a function of the applied spatial force, $\mathbf{f}_B = \left[\boldsymbol{n}_B^T,\ \boldsymbol{f}_B^T\right]^T$, by

$$\mathbf{a}_B = (\boldsymbol{I}_B^A)^{-1}\mathbf{f}_B + {}^B\mathbf{X}_E\,\mathbf{a}_g \tag{2}$$

where $\boldsymbol{I}_B^A$ is the articulated body inertia of the body, ${}^B\mathbf{X}_E$ is the spatial transform from earth coordinates to body coordinates, and $\mathbf{a}_g = [0,\ 0,\ 0,\ 0,\ 0,\ -9.81]^T$ is the gravity vector in earth coordinates.

The applied spatial force, $\mathbf{f}_B$, is resolved as a function of system torque, $\boldsymbol{\tau} = [\boldsymbol{\tau}_1^T,\ \boldsymbol{\tau}_2^T,\ \boldsymbol{\tau}_3^T,\ \boldsymbol{\tau}_4^T]^T$, by

$$\mathbf{f}_B = \bar{\mathcal{J}}^T\boldsymbol{\tau} + \mathbf{b}_B^A\ . \tag{3}$$

where $\mathbf{b}_B^A$ is the articulated velocity-dependent bias term computed as the sum of the body's bias term, $\mathbf{b}_B$, and each leg's articulated bias term, $\mathbf{b}_\ell^A$:

$$\mathbf{b}_B^A = \mathbf{b}_B + \sum_{\ell=1}^{4}\mathbf{b}_\ell^A\ . \tag{4}$$

In Eq. 3,

$$\bar{\mathcal{J}}^T = \left[\bar{\mathcal{J}}_1^T,\ \bar{\mathcal{J}}_2^T,\ \bar{\mathcal{J}}_3^T,\ \bar{\mathcal{J}}_4^T\right] \tag{5}$$

where $\bar{\mathcal{J}}_\ell$ is the dynamically-consistent generalized inverse of the Jacobian matrix for leg ℓ [20]. An efficient algorithm has been developed for computing $\bar{\mathcal{J}}$. Its formulation is not presented here because of space limitations, but will be included in future publications.

Using Eqs. 2 and 3, the acceleration of the body can be computed from the system's 12 joint torques. In predicting the passive dynamics of the system, the SLIP model does not consider the dynamic effects of the flight legs, which cause a significant disturbance when protracting forward at high speed [16]. Further, only axial leg thrusts (knee torques for our system) of the stance legs are present in the SLIP analysis; hip torques are assumed to be zero. The SLIP spatial force, $\tilde{\mathbf{f}}_B$, of the passive system is based solely on the knee torques from the passive springs and resulting spatial forces of the stance legs. Assuming that legs 1 (front left) and 4 (back right) are on the ground, then the subsequent body accelerations, $\tilde{\mathbf{a}}_B$, can be computed thereafter by

$$\tilde{\mathbf{f}}_B = \left[\bar{\mathcal{J}}_1^T,\ \bar{\mathcal{J}}_4^T\right] \begin{bmatrix} \boldsymbol{\tau}_1^o \\ \boldsymbol{\tau}_4^o \end{bmatrix} + \mathbf{b}_B + \mathbf{b}_1^A + \mathbf{b}_4^A \ , \text{ and} \tag{6}$$

$$\tilde{\mathbf{a}}_B = (\boldsymbol{I}_B^A)^{-1}\tilde{\mathbf{f}}_B + {}^B\mathbf{X}_E\, \mathbf{a}_g \ , \tag{7}$$

where

$$\boldsymbol{\tau}_\ell^o = [0,\ 0,\ \tau_{\ell,k}^o] \qquad \ell = 1, 4 \ . \tag{8}$$

For a stance leg, $\tau_{\ell,k}^o$ is the knee torque produced by the passive knee spring.

The force redistribution algorithm seeks to preserve the passive SLIP dynamics by setting the desired body accelerations, a_B^d, to the SLIP accelerations for the forward, lateral, vertical, and yaw motions:

$$\begin{aligned} \mathrm{a}_B^{x,d} &= \tilde{\mathrm{a}}_B^x \\ \mathrm{a}_B^{y,d} &= \tilde{\mathrm{a}}_B^y \\ \mathrm{a}_B^{z,d} &= \tilde{\mathrm{a}}_B^z \\ \mathrm{a}_B^{\alpha,d} &= \tilde{\mathrm{a}}_B^\alpha \ . \end{aligned} \tag{9}$$

The desired body accelerations for the roll and pitch axes are servo-controlled to a desired position and rate:

$$\begin{aligned} \mathrm{a}_B^{\gamma,d} &= k_\gamma(\gamma_d - \gamma) + k_{\dot{\gamma}}(\dot{\gamma}_d - \dot{\gamma}) \\ \mathrm{a}_B^{\beta,d} &= k_\beta(\beta_d - \beta) + k_{\dot{\beta}}(\dot{\beta}_d - \dot{\beta}) \ , \end{aligned} \tag{10}$$

where k_γ, $k_{\dot{\gamma}}$, k_β, and $k_{\dot{\beta}}$ are control gains. Expanding Eq. 3 and substituting into Eq. 2 with the desired body accelerations now on the left hand side yields

$$\begin{aligned} \mathbf{a}_B^d = (\boldsymbol{I}_B^A)^{-1}\Bigg(& \left[\bar{\mathcal{J}}_1^T,\ \bar{\mathcal{J}}_4^T\right] \begin{bmatrix} \boldsymbol{\tau}_1 \\ \boldsymbol{\tau}_4 \end{bmatrix} \\ & + \left[\bar{\mathcal{J}}_2^T,\ \bar{\mathcal{J}}_3^T\right] \begin{bmatrix} \boldsymbol{\tau}_2^o \\ \boldsymbol{\tau}_3^o \end{bmatrix} + \mathbf{b}_B^A \Bigg) + {}^B\mathbf{X}_E\, \mathbf{a}_g \ . \end{aligned} \tag{11}$$

For flight legs 2 (front right) and 3 (back left), τ_ℓ^o consists of the current applied torques to shorten, protract, and lengthen the legs during transfer. Algebraic manipulation of Eq. 11 leads to

$$\begin{aligned} \left[\bar{\mathcal{J}}_1^T,\ \bar{\mathcal{J}}_4^T\right] \begin{bmatrix} \boldsymbol{\tau}_1 \\ \boldsymbol{\tau}_4 \end{bmatrix} = \boldsymbol{I}_B^A\, (\mathbf{a}_B^d - {}^B\mathbf{X}_E\, \mathbf{a}_g) \\ - \left[\bar{\mathcal{J}}_2^T,\ \bar{\mathcal{J}}_3^T\right] \begin{bmatrix} \boldsymbol{\tau}_2^o \\ \boldsymbol{\tau}_3^o \end{bmatrix} - \mathbf{b}_B^A \ . \end{aligned} \tag{12}$$

This equation computes torques for legs 1 and 4 which will now include hip torques and an adjusted knee torque. The actuator on the thigh can adjust the rest position of the series spring element to deliver the necessary change in torque at the knee. Note that similar equations can be developed when legs 2 and 3 are on the ground.

The 6x6 matrix, $[\bar{\mathcal{J}}_1^T,\ \bar{\mathcal{J}}_4^T]$, is ill-conditioned as expected based upon the previous discussion that only five elements of body motion can be independently controlled. Singular value decomposition (SVD) techniques can solve this set of equations and return values for $\boldsymbol{\tau}_1$ and $\boldsymbol{\tau}_4$ that minimize the errors between the desired and achievable forces [21]. Weights can be integrated into the SVD computation to prioritize the accuracy of the controller on selected motion elements. Roll and pitch motions are prioritized to maintain level trotting, resulting in increased errors of the four SLIP motions. Only lateral velocity showed any significant effects from this choice of priorities, but this does not disturb the system enough to cause instability even at high speeds. It is expected that the fuzzy algorithm in the step controller performs better when the body tilt angles are predictable and repeatable during stance, which is the reason to give priority to roll and pitch motions.

IV. Results

The control algorithm was tested in RobotBuilder [22], a robot simulation environment built upon the DynaMechs [23] dynamics engine for general robotic systems. System losses are modeled as damping in the compliant ground. Ground spring and damping coefficients are $75\ kN/m$ and $2\ kN/m/s$ respectively. Ground static and kinetic friction coefficients are 0.75 and 0.6 respectively, matching the properties of rubber on concrete.

Figure 7 shows the response of the quadruped to changes in desired speed and turning rate. Acceleration is limited to $0.25\ m/s$ per step, allowing the quadruped to increase velocity by $1\ m/s$ in four steps. The turning rate can increase or decrease by $10\ deg/s$ in one step. During the first 50 steps, the control system accelerates the body to $4.0\ m/s$. Yaw rate is well controlled at low speeds, but becomes more difficult to control at higher speeds. Although the top speed for straight-line running is $4.75\ m/s$, turning at significant rates cannot be controlled at that speed. Turning results are shown here at $3.0\ m/s$.

Figure 8 shows selected body states through five steps, lettered A-E. The shaded areas represent the periods of support for a diagonal pair. During support phase A, the velocity and height respond similarly to what is observed in nature and predicted by the SLIP model, as was shown in

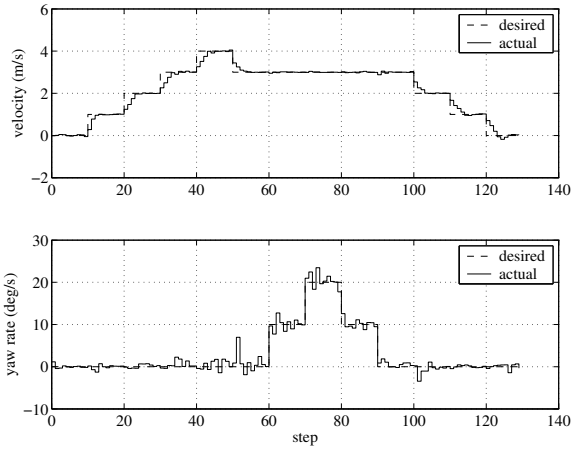

Fig. 7. Tracking of velocity and turning rate.

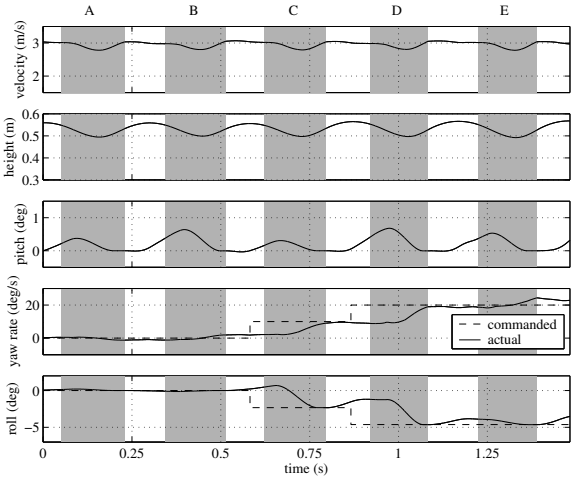

Fig. 8. The forward and vertical dynamics of the body are similar for each step, regardless of the pitch and roll correction done during the shaded support phases.

Fig. 2. The pitch, which is increasing away from zero at the moment of contact, is controlled back to zero before liftoff occurs. Neither yaw rate nor roll move significantly away from their desired values during the first step.

After a leg finishes its support phase and breaks contact with the ground, torque is applied to its swing axis to protract the leg forward to the touchdown position. This torque exerts a positive (nose-down) pitching moment on the body, which goes unopposed because the body is largely uncontrollable during flight. The legs must begin protracting forward during flight because only a limited amount of time is available before the leg must be in position for its next touchdown. The pitch motion can be observed diverging from zero between support phase A and support phase B. The flight legs continue to swing forward during support phase B, but the force redistribution algorithm overcomes this disturbance to control the pitch back to zero. Raibert observed the same nose-down pitching due to protracting legs [3], but his pitch control algorithm during stance was unable to fully eliminate the error.

During the flight period between support phase B and support phase C, the user changes the desired yaw rate to $10\ deg/s$. The desired roll angle immediately changes to the bank angle corresponding to that forward velocity and turning rate. During support phase C, the force redistribution algorithm simultaneously corrects roll and pitch without much disturbance to the forward and vertical dynamics. The change in yaw rate is a function of the ab/ad angles at touchdown, which are outputs of the fuzzy controller. During support phase D, a faster turning rate dictates a larger bank angle, which is maintained during the following support phase E. Notice that the forward and vertical dynamics are similar for each of the five steps, mostly impervious to the changes in stance control effort for roll and pitch motion.

Figure 9 shows the fundamental value of this control algorithm. The system is initialized at three different pitch values at TOF: $4.0\ deg$, which is significantly larger than what the controller expects to correct during normal trotting, $1.0\ deg$, which is the expected pitch correction for a typical step, and $0.0\ deg$, which requires minimal correction during stance. The quadruped trot exhibits minimal pitch oscillations in nature, so another gait or foot sequence may be used when tilt errors above $4.0\ deg$ occur. During the support phase (shaded), the pitch is controlled to zero in all cases. The forward and vertical motions during the steps are also shown. Pitch motion is prioritized to achieve its goal, but at the expense of forward velocity. The dynamics of a passive system as predicted by the SLIP model are displayed during the case of minimal pitch correction.

The force redistribution algorithm is capable of eliminating the $4.0\ deg$ of pitch error, but the velocity during this step deviates from the passive system. The loss of velocity can be corrected during the next step, during which more reasonable pitch error will exist. Figure 8 shows the expected pitch error for one step to be approximately $0.5\ deg$, so the pitch error of $1.0\ deg$ in Fig. 9 is more likely, and is eliminated without significantly affecting the body's forward motion. In neither case was the body's vertical motion disturbed, revealing that vertical motion does not have much dependency on pitch motion. Roll and lateral velocity have a similar dependency to what is observed here between pitch and forward velocity, but the body's lateral sway remains manageable during high-speed running and turning.

V. Summary and Future Work

Simulation results are presented for the control of a 3D quadruped running trot. The controller attempts to preserve the nominal passive dynamics of quadruped trotting. In doing so, it is expected (although not proven here) that this controller enjoys energy optimality over controllers that overpower the natural dynamics. The controller was shown to perform well accelerating the quadruped to and maintaining high running speeds, and was stable enough to handle the added difficulty of turning. A hybrid control strategy is presented which allows the quadruped to reach a speed of $4.75\ m/s$ and turn at a rate of $20\ deg/s$ under operator control. The *discrete* part of the controller runs

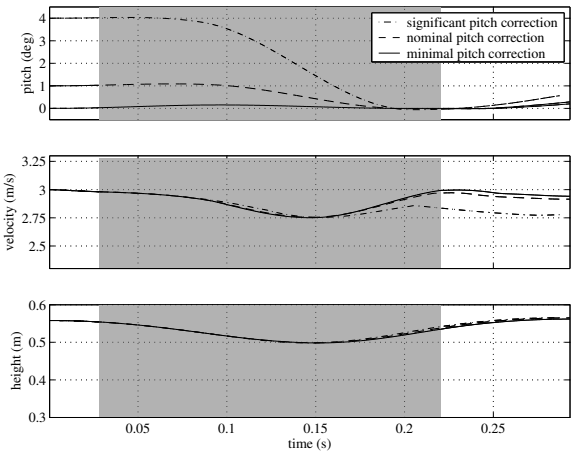

Fig. 9. Pitch, velocity, and height variation over one step for three different values of initial pitch error.

once per trot step and outputs a stance thrust energy and hip angles for touchdown. Both the stance thrust energy and hip angles dictate the natural dynamics during stance. The force redistribution algorithm *continuously* operates during the support phase to stabilize the body's tilt axes, roll and pitch, with minimal effect on the prescribed natural dynamics. The controller also tracks desired changes in heading, for which the biomimetic method of banking into a high-speed turn is also realized.

Simulation of robotic systems is useful for the hardware and control system design of experimental robots. Control algorithms can be analytically studied and easily modified in simulation to identify useful control principles or to verify the viability of a control method. Once a proof of concept is completed for an algorithm, some of the computational complexities of the algorithm can be simplified to run on a real-time system. This paper verifies the effectiveness of the controller, but the computation of the dynamically-consistent generalized inverse of the Jacobian matrix for leg ℓ, $\bar{\mathcal{J}}_\ell$, may be too complex to compute in real time. Computing the standard Jacobian requires less computation and can be inserted into the algorithm without a significant reduction in the controller performance. Results in this area will be the subject of future publication.

Further work will also investigate the energy optimality of this control method when compared to other methods being used. Verifying that biomimicry has energetic advantages would be a significant contribution to the study of high-speed legged locomotion. The effectiveness of this control algorithm over irregular terrain will also be studied.

ACKNOWLEDGMENTS

Support was provided by grant no. IIS-0535098 from the National Science Foundation to The Ohio State University, and through a teaching associateship in the Department of Electrical and Computer Engineering at The Ohio State University.

REFERENCES

[1] D. F. Hoyt and C. R. Taylor, "Gait and the energetics of locomotion in horses," *Nature*, vol. 292, pp. 239–240, 1981.
[2] R. M. Alexander, "The gaits of bipedal and quadrupedal animals," *International Journal of Robotics Research*, vol. 3, pp. 49–59, 1984.
[3] M. H. Raibert, "Trotting, pacing, and bounding by a quadruped robot," *Journal of Biomechanics*, vol. 23, suppl. 1, pp. 79–98, 1990.
[4] I. Poulakakis, J. A. Smith, and M. Buehler, "On the dynamics of bounding and extensions towards the half-bound and the gallop gaits," in *Proceedings of the 2^{nd} International Symposium on Adaptive Motion of Animals and Machines*, (Kyoto, Japan), March 2003.
[5] P. Nanua and K. J. Waldron, "Energy comparison between trot, bound, and gallop using a simple model," *Journal of Biomechanical Engineering*, vol. 117, pp. 466–473, November 1995.
[6] P. P. Gambarian, *How Mammals Run*. New York, NY: John Wiley & Sons, 1974.
[7] G. A. Cavagna, N. C. Heglund, and C. R. Taylor, "Mechanical work in terrestrial locomotion: two basic mechanisms for minimizing energy expenditure," *American Journal of Physiology*, vol. 233, no. 5, pp. R243–R261, 1977.
[8] R. J. Full and C. T. Farley, *Musculoskeletal Dynamics in Rhythmic Systems: A Comparative Approach to Legged Locomotion*. New York: Springer Verlag, 2000.
[9] R. M. Alexander, *Elastic Mechanisms in Animal Movement*. Cambridge: Cambridge University Press, 1988.
[10] R. Blickhan and R. J. Full, "Similarity in multilegged locomotion: Bouncing like a monopode," *Journal of Comparative Physiology A*, vol. 173, pp. 509–517, 1993.
[11] A. Goswami, B. Espiau, and A. Keramane, "Limit cycles and their stability in a passive bipedal gait," in *Proceedings of the IEEE International Conference on Robotics and Automation*, (Minneapolis, MN), pp. 246–251, April 1996.
[12] H. M. Herr and T. A. McMahon, "A trotting horse model," *International Journal of Robotics Research*, vol. 19, pp. 566–581, June 2000.
[13] L. R. Palmer III, *Control of a High-Speed Quadruped Trot*. PhD thesis, The Ohio State University, 2007.
[14] D. V. Lee, J. E. A. Bertram, and R. J. Todhunter, "Acceleration and balance in trotting dogs," *Journal of Experimental Biology*, vol. 202, pp. 3565–3573, 1999.
[15] K. Yoneda, H. Iiyama, and S. Hirose, "Sky-hook suspension control of a quadruped walking vehicle," in *Proceedings of the IEEE International Conference on Robotics and Automation*, (San Diego, CA), pp. 999–1004, 1994.
[16] L. R. Palmer III and D. E. Orin, "Attitude control of a quadruped trot while turning," in *Proceedings of the International Conference on Intelligent Robots and Systems (IROS)*, (Beijing, China), pp. 5743–5749, October 2006.
[17] L. R. Palmer III and D. E. Orin, "3D control of a high-speed quadruped trot," *Industrial Robot*, vol. 33, no. 4, pp. 298–302, 2006.
[18] R. Featherstone, "The calculation of robot dynamics using articulated-body inertias," *The International Journal of Robotics Research*, vol. 2, no. 1, pp. 13–30, 1983.
[19] W. Hu, D. W. Marhefka, and D. E. Orin, "Hybrid kinematic and dynamic simulation of running machines," *IEEE Transactions on Robotics*, vol. 21, pp. 490–497, June 2005.
[20] O. Khatib, "A unified approach for motion and force control of robot manipulators: the operational space formulation," *IEEE Transactions on Robotics and Automation*, vol. RA-3, pp. 43–53, February 1987.
[21] W. H. Press, S. A. Teukolsky, W. T. Vetterling, and B. P. Flannery, *Numerical recipes in C++*. New York, NY: Cambridge University Press, second ed., 2002.
[22] S. J. Rodenbaugh, "RobotBuilder: A graphical software tool for the rapid development of robotic dynamic simulations," Master's thesis, The Ohio State University, Columbus, Ohio, 2003.
[23] S. McMillan, D. E. Orin, and R. B. McGhee, "DynaMechs: An object oriented software package for efficient dynamic simulation of underwater robotic vehicles," in *Underwater Robotic Vehicles: Design and Control*, pp. 73–98, Albuquerque, NM: TSI Press, 1995.